Electronic Lock-in Amplifier for Low Cost Radiation Thermometry

Samuel Maxwell[1]

***Abstract* — Radiation Thermometry encompasses instruments that measure Black Body radiation to calculate an object's surface temperature. Measurement of Black Body radiation requires highly sensitive detectors due to the low optical power of the emitted light producing input signals in the order of nA, especially at measurement distances greater than 1m. Pre-modulation of the input signal allows measurement using Phase Sensitive Detection, eliminating noise contributions from front-end amplifiers. This paper reports the design, implementation and testing of a fully electronic Lock-in Amplifier (LIA) for measuring low optical powers in the near Infrared spectrum. Here we show the system is capable of measurement down to 740°C, with significant improvement attainable through further testing, at a total cost less than £100 in a small form factor. This shows it is possible to produce highly sensitive Lock-in Amplifiers at a fraction of the cost and size of commercially available equipment. Thus, it is possible to use this Phase Sensitive Detection technology in more prevalent optical applications such as Radiation Thermometry, Fibre-optic Communications and LIDAR; where previously, mechanical considerations and cost would have been a barrier to entry.**

***Index Terms* — Arduino, Lock-in Amplifier, Phase Sensitive Detection, Photodiode, Python, Radiation Thermometry, Transimpedance Amplifier.**

I. Introduction

Accurate and repeatable temperature measurement is a key requirement in many industrial sectors, including the Chemical, Pharmaceutical and Steel Industries [1]. Factories rely upon reliable temperature measurements to regulate key manufacturing systems such as Curing Ovens and Furnaces. At present, Contact Thermometers are the most widely used temperature measurement device in industry due to their ease of installation, accuracy of measurement and low cost. Unfortunately, high temperature environments greatly reduce a Contact Thermometer's accuracy of measurement, due to interfering radiation from other sources heating the detector [2]. Thus, the device produces a reading that is the average of the contacted surface and environmental temperature [2].

Radiation Thermometers provide a solution to this problem by measuring the emitted Infrared radiation from the desired source to calculate the surface temperature. The Thermometer can be placed outside the system being measured, mitigating the effects of a high temperature environment [2]. Most devices also incorporate optics to focus their cone of detection onto a small section of the source's surface, further reducing interference from external radiation sources.

[1]This 3rd year Individual Project was performed at the Department of Electronic & Electrical Engineering at the University of Sheffield, UK It was supervised by Professor Chee Hing Tan (e-mail: c.h.tan@sheffield.ac.uk).

PN or PIN Photodiodes are the most common detectors in current industrial Radiation Thermometers. Devices with a larger Radiant Sensitive Area (the area of the Photodiode that is sensitive to incident photons) are selected to maximize the spectral power contacting the detector. Unfortunately, this increases the devices' cone of detection, resulting in the measurement of the average temperature of a section of the source's surface instead of an ideal single point measurement [2]. Single point measurements are desirable as they increase the resolution of source surface temperature scans.

In practice, output signals from Photodiodes are in the order of nA, due to the limited maximum Radiant Sensitive Area of devices and larger measurement distances reducing optical power. Low-noise, high sensitivity detection circuitry is required to accurately measure these signals where interference may be of a comparable magnitude.

Modulation of the low power optical input signal using an Optical Chopper [3] allows the use of Lock-in Amplifiers (a form of Phase Sensitive Detection) for measurement [4] [5]. A typical setup for this method is shown in Fig. 1. Lock-in Amplifiers (LIA) can extract an input signal from a noise floor upwards of 100dB [6]. The greater the detection sensitivity, the smaller the Radiant Sensitive Area of the Photodiode can be, pushing the cone of detection towards a single point measurement.

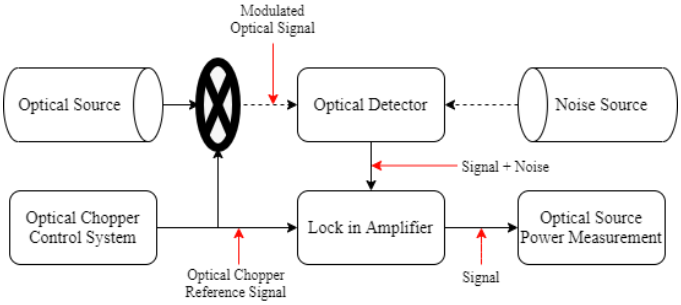

Figure 1: Optical Chopper Measurement Setup Diagram

Unfortunately, this setup is not viable for most commercial applications due to its cost and mechanical constraints. Typical commercial LIAs cost upwards of £1000 [7] and Optical Choppers require expensive calibration and maintenance to ensure they provide accurate modulation.

This paper documents the development of a low-cost, fully electronic Lock-in Amplifier for use in Radiation Thermometry applications. To remove the problems caused by mechanical components, an electronic modulation circuit with two Photodiodes replaces the Optical Chopper, as shown in Fig. 2. One Photodiode detects radiation from the target source and the other acts as a dark current reference channel. Additionally, we aim to quantify the suitability of Electronic LIAs for Radiation Thermometry applications.

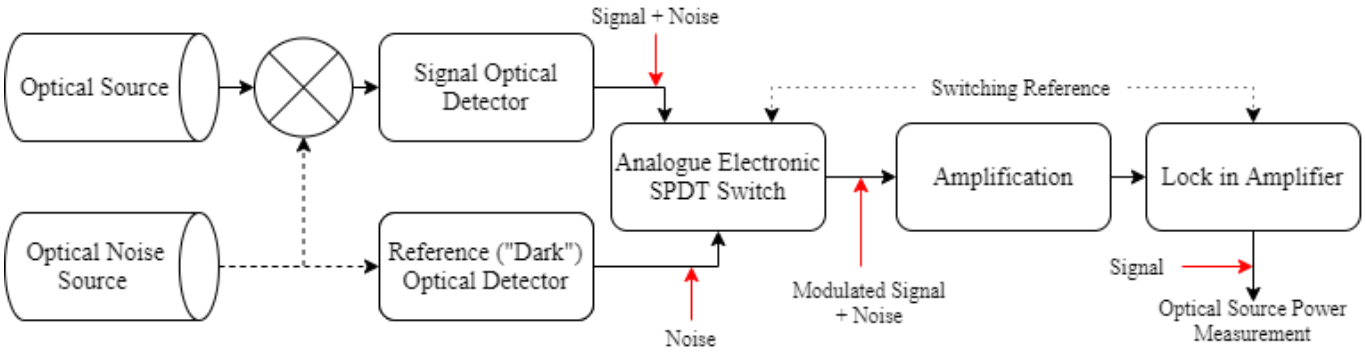

Figure 2: Electronic Lock-in Amplifier System Diagram

A. *Project Specification*

The specification for this project, taken from the Interim Report [8], is as follows:

1) Explore the use of Electronic Lock-in Amplifiers for Radiation Thermometry by performing test measurements with existing hardware created by Tarick Osman [9].
2) Improve the existing circuit to detect below nA, aiming for pA.
   - Construct a new Low Noise Transimpedance Amplifier (TIA) with a gain to facilitate measurements in the pA range.
   - Construct an Electronic Lock-in Amplifier with a filter appropriate for Radiation Thermometry.

B. *Black Body Radiation*

All objects above a uniform temperature of 0K emit Electromagnetic Radiation, usually from the Infrared and Visible spectrums between 0.5µm and 20µm [2] [8]. This is referred to as Black Body Radiation. Black Bodies are idealized objects that perfectly absorb and emit radiation. Unfortunately, no perfect Black Bodies exist in the real world [2]. Black Body radiation has a characteristic frequency spectrum that changes with temperature, as shown in Fig. 3.

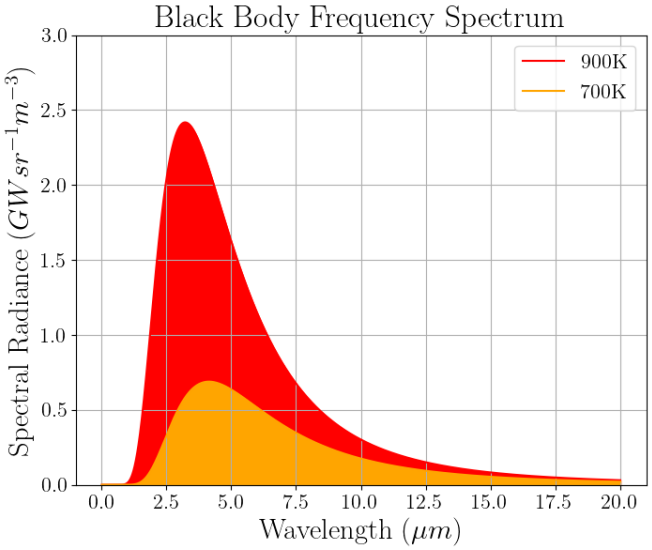

Figure 3: Example Black Body Frequency Spectrum at 700K and 900K

The wavelength of peak Spectral Radiance for a Black Body at a given temperature can be calculated using (1), Wein's Law. Additionally, the Stefan-Boltzmann Law (2) can be used to calculate the total Spectral Radiance for a Black Body at a given temperature.

$$\lambda_{max} = \frac{2898}{T}\mu m \tag{1}$$

$$M = \varepsilon\sigma T^4\ Wsr^{-1}m^{-2} \tag{2}$$

More information on Black Body Radiation and how it is used in Radiation Thermometry can be found in the project Interim Report [8].

C. *Transimpedance Amplifiers*

Transimpedance Amplifiers (TIA) convert current-based input signals, such as those produced by Photodiodes, to voltage-based output signals. A typical Transimpedance Amplifier circuit with a Photodiode model is shown in Fig. 4 [10], [11].

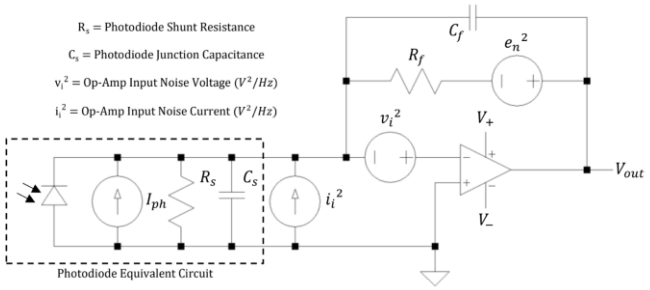

Figure 4: Transimpedance Amplifier with Noise Equivalent Circuit and Photodiode Model

Equation (3) and (4) give the Transimpedance Gain and Corner Frequency of the Transimpedance Amplifier shown in Fig. 4 [6].

$$\frac{V_{out}}{I_{in}} = -\frac{R_f}{j\omega C_f R_f + 1}\ \Omega \tag{3}$$

$$f_c = \frac{1}{2\pi C_f R_f}\ Hz \tag{4}$$

To prevent oscillation, a sufficiently large feedback capacitor (C_f) is placed in parallel with the feedback resistor (R_f). This counteracts the second order response introduced by the Photodiode capacitance (C_s) [11].

Transimpedance Amplifiers are the most used Input Stage for Photodiode circuits. Consequently, it is important to ensure the TIA does not introduce large amounts of noise to the signal in order to maximize signal to noise ratio. Johnson Noise, Shot Noise and Flicker Noise all contribute to the noise of a TIA [6]; their contributions are modelled in Fig. 4. It is important to limit each contribution as much as possible; however, in most cases this forms a tradeoff between different types of noise.

More information on Transimpedance Amplifiers and the different noise tradeoffs can be found in the project Interim Report [8].

D. Lock-in Amplifiers and Phase Sensitive Detection

Lock-in Amplifiers employ Phase Sensitive Detection to extract signals of a specific frequency from noise [4]. A modulated input signal and reference signal at the same frequency (the reference frequency) are mixed (multiplied) [4]. This produces a signal at DC and harmonics of the reference frequency, when a square wave reference is used. The input signal modulation can be performed using an electronic switch or Optical Chopper as discussed previously.

Low Pass filtering of the mixer output signal produces a DC voltage proportional to the amplitude of the input signal, as described in (5) [4], [6].

$$Output\ DC\ Signal\ \approx \frac{664 V_s V_R}{75\pi^2}\ V \qquad (5)$$

To produce the greatest amplitude of output, the input signal and reference signal should be in phase. Many Lock-in Amplifiers incorporate Phase Locked Loops (PLLs) to achieve this [4]. A systems diagram for Phase Sensitive Detection is shown in Fig. 5.

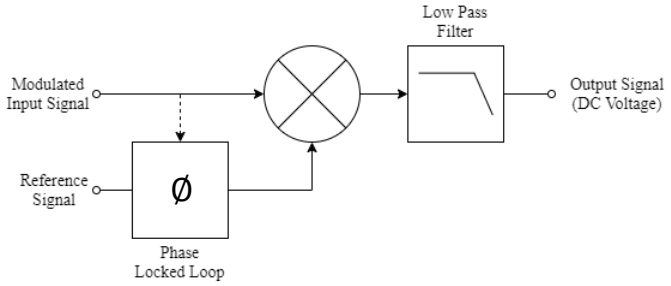

Figure 5: Phase Sensitive Detection Systems Diagram

Phase Sensitive Detection is a powerful method of measurement as it removes all noise sources apart from those at the same frequency as the reference signal. This is useful in Photodiode front end circuits, where the signal to noise ratio can be relatively low.

More information on LIAs and Phase Sensitive Detection can be found in the project Interim Report [8].

II. Economic, Legal, Social, Ethical and Environmental Context

Photodiode detection circuitry has a wide range of applications in modern engineering, including Fibre-optic Communications, Autonomous Vehicles (LIDAR) and Temperature Measurement. Applications in LIDAR and Communications have become increasingly important as we move towards an autonomous, digital world.

Fibre-optic communications are poised to become a vital part of the UK's infrastructure, with the government pledging £5 Billion to ensure implementation in hard to reach areas [12]. High speed communication brings several benefits for businesses and public services, including increased home-working productivity, new business opportunities through remote collaboration and more efficient online services [12]. OFCOM research shows that broadband investment has significantly contributed to the UK economy [13].

Contrastingly, applications of LIDAR technology have generated significant public controversy, largely through crashed autonomous vehicles. Crashes caused by Tesla's Autopilot system [14] have drawn continuous scrutiny of the safety surrounding autonomous vehicle technologies. Development in the technological, legal and ethical areas of autonomous systems is required for these products to properly integrate with society.

III. Methodology

This section provides a summary of the design and implementation of key sections of the Lock-In Amplifier including the Transimpedance Amplifier (TIA), Lock-in Amplifier (LIA) IC, Final Circuit Board and Control Software. For more detailed information please consult the project Interim Report [8].

A. Photodiode Selection

Selection of an appropriate Photodiode is extremely important for this design; a poorly selected device could introduce large amounts of noise or cause oscillations in the Transimpedance Amplifier stage [6]. The following are requirements for the Photodiode.

Firstly, a device with a large Radiant Sensitive Area should be selected whilst attempting to maintain a reasonable Junction Capacitance [15].

Secondly, a device with a small Dark Current should be selected. The Dark Current acts as a noise floor, limiting the minimum optical power that can be measured [15]. Ideally, the Lock-in Amplifier will remove the Dark Current signal contribution. However, differences in Photodiode Dark currents due to manufacturing tolerances mean it is beneficial to limit Dark Current where possible.

Based upon these requirements, the OSRAM SFH2200 PIN near Infrared Photodiode [16] was selected for the design.

B. Transimpedance Amplifier Design

Based upon the previously discussed theory [8], several requirements can be stipulated for the design of a low noise Transimpedance Amplifier.

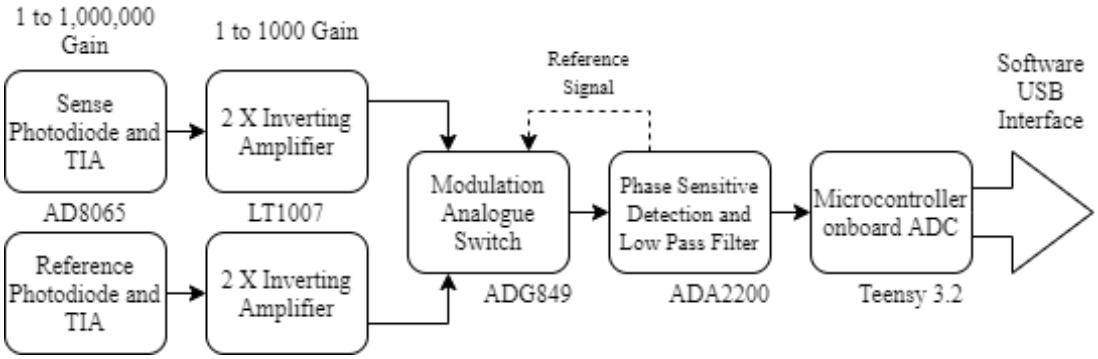

Figure 6: Lock-in Amplifier Top Level System Diagram

Firstly, the selected operational amplifier should have a small input bias current and input noise current [6]. Both values will be amplified by the TIA and directly affect the signal to noise ratio of the circuit.

Secondly, the selected operational amplifier should have a small input noise voltage. This noise interacts with the operational amplifiers input capacitance to produce a noise that is also amplified by the TIA [6].

Thirdly, an operational amplifier with a low flicker noise at DC should be selected [6]. As flicker noise increases with decreasing frequency, this is important.

Finally, as the circuit operates at DC, as high a value of R_f as possible should be used [17]. The noise current produced by the feedback resistor will be amplified by the TIA; using a large feedback resistor value ensures that this noise current is minimized. This will decrease bandwidth, with the benefit of increased transimpedance gain [17].

Based upon these requirements a list of candidate operational amplifiers, shown in Table I, was created. Each of these operational amplifiers was then simulated using Analog Devices LT SPICE [10] to provide frequency, linearity and noise responses. A feedback resistance of 100kΩ and feedback capacitance of 1.5nF were selected to produce a TIA with a transimpedance gain of 100k and bandwidth of 1kHz. These values were calculated using (3) and (4) and are representative of potentially desired values for the final circuit implementation.

Using the results of the simulation, the AD8065 and AD795 were selected for further practical testing. The simulated circuits were replicated and tested for frequency and linearity.

C. Phase Sensitive Detection Circuitry Design

In order to simplify the design process for the Lock-in Amplifier the Analog Devices ADA2200 [18] was selected to implement the Phase Sensitive Detection section of the circuit. This IC provides the mixing functionality required for Phase Sensitive Detection and can easily be combined with a Low Pass Filter (LPF) to implement a basic Lock-in Amplifier.

In addition to this basic functionality, the ADA2200 provides several other features of use to a Lock-in Amplifier design. A set of configurable clock dividers are available internally, providing all required frequencies for the IC from one master input clock signal [18].

The reference clock generated by the IC can be shifted by 90° in phase, allowing for both In Phase and Quadrature measurements of the input signal [18]. These two readings can be combined to produce an output that is independent of the phase difference between the input signal and reference signal.

Finally, an Infinite Impulse Response (IIR) and Decimation Filter are provided internally [18]. The coefficients of the IIR filter are fully programmable via the ADA2200 SPI interface.

D. Lock-in Amplifier System Structure

Fig. 6 shows the top-level systems diagram for the Lock-in Amplifier as implemented in the final version of the PCB. Additionally, Fig. 16 in the Appendix shows the complete schematic for the Lock-in Amplifier PCB.

Two separate Photodiode channels are used, one for sensing and one as a reference. Modulating between a signal and a reference channel ensures the Photodiode dark current is removed from the signal by the Lock-in Amplifier, providing a more accurate measurement of the light hitting the sensing channel Photodiode.

Each channel has a TIA and two Inverting Amplifiers before the modulation and phase sensitive detection sections of the circuit. The Inverting Amplifiers are implemented using the LT1007 [19]. This provides a maximum of 1 Billion gain before the Lock-in Amplifier, allowing amplification of pA signals to the mV range. This is required as the ADA2200 takes input signals from 0.3 to 3.3V [18].

Modulation is implemented using an ADG849 analogue switch (U10) [20]. The reference signal for modulation is provided directly from the ADA2200 RCLK pin, its frequency can be configured using the two internal clock dividers. A second ADG849 (U4) is used to multiplex the RCLK pin as it is also used for SPI communications.

Placing the modulation stage after all amplification stages allows for much higher reference signal frequencies to be used as the bandwidth is not limited by the TIA or Inverting Amplifiers.

The ADA2200 (U13) is configured as per the datasheet Lock-in Amplifier application guidance [18]. Connections for SPI communications have been implemented so that the internal IIR filter and clock dividers can be configured. Three LPF configurations with corner frequencies of 1.6, 0.16 and 0.016Hz are provided on the ADA2200 output, allowing for a wider range of reference frequencies to be used. The SYNCO (Sync out) pin is connected to the Microcontroller, allowing the firmware to trigger an ADC read when the LIA output is stable [18].

A Teensy 3.2 Microcontroller (U12) is also included in the design to allow for software control and logging of the Lock-

in Amplifier. This development board provides a 32-bit Cortex-M4 processor clocked at 72MHz and a 16-bit ADC [21]. Software implementation of Digital Signal Processing techniques is possible due to the processor's high clock speed. The 16-bit ADC improves the granularity of measurement over the previous design [9], giving 50.35µV resolution over a 3.3V range.

An LM2937 Linear Voltage Regulator (U1) [22] has been implemented to provide the 3.3V power supply rail. This is supported by Zener diodes for over-voltage protection on the 5V rails. Additionally, a set of tactile switches and a connector for an 8-bit parallel LCD have been provided for convenience. They are not currently supported in firmware.

E. PCB Design

Schematic capture and PCB layout was completed using KiCAD [23]. This design aims to minimize the noise introduced to the analogue section of the circuit from the digital section and external sources. Appendix Fig. 17 shows a render of the completed design.

100pF and 100nF bypassing capacitors are placed across all power supply pins of ICs to negate the effects of power supply ripple. These capacitors are placed physically as close to the ICs as possible. The 5V and -5V supply rails have a 10µF bypass capacitor to further smooth ripple [24].

The analogue and digital sections are kept as far apart as possible and have a split ground plane that connects at the 5V/-5V input connector [24]. This reduces interference from switching digital signals in the analogue circuit. The ground plane is stitched with vias, appearing on both sides of the PCB. This decreases the size of ground loops, limiting stray inductance and producing a common ground reference [24].

1206 SMD passive components were used to provide small, hand-solderable packages that could be tightly placed. Analogue ICs were placed close together to limit parasitic inductance and capacitance. Where analogue and digital signals had to overlap, they were routed perpendicular to each other on either side of the board; this limits inductance coupling.

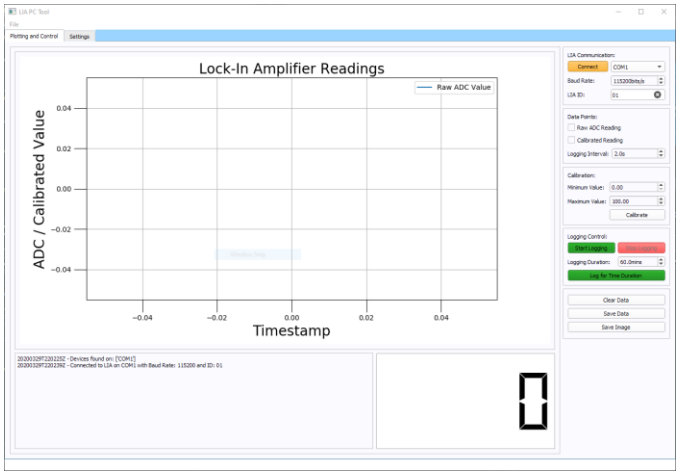

Figure 7: LIA PC Tool Plotting and Control Tab

F. LIA Control Software and PC Tool

Alongside hardware development for the Lock-in Amplifier, software (PC Tool) and firmware (Control Software) was implemented to provide settings configuration and granular logging of the Lock-in Amplifier.

Fig. 7 shows the logging page of the PC Tool. The tool aims to provide easy-to-use logging and settings configuration for the Lock-in Amplifier via a Graphical User Interface (GUI) and USB connection. The PC Tool was written in the Python programming language using the QT Graphics library, allowing for rapid development and expandability as well as simpler data handling and visualization.

The Control Software (running on the Microcontroller), written in the Arduino programming language, performs the routines required to make measurements and change settings on the Lock-in Amplifier PCB.

A custom text-based protocol was developed to link the PC Tool and Control Software. The PC Tool sends commands using this protocol, which the Control Software then reads and executes. More information on this protocol can be found in the Remote Communication Protocol guide [25]. The software can be found in the project Github repository [26].

G. Case and Mounting Hardware

To provide protection and accessible mounting of the Lock-in Amplifier to optical tables, a case was developed for the final circuit board; Fig. 18 (see Appendices) shows the manufactured case. The case was designed specifically for rapid prototyping using Additive Manufacturing technology.

Access to all connectors and buttons is provided through the top plate or case side. The light guide provides an easy way to cover one Photodiode to act as a reference channel. A mounting plate and holes have been placed on the rear to allow easy screwing or clamping to an optical table.

H. Black Body Source Testing Setup

To provide a benchmark for evaluating the performance of both the previous design [9] and new design, a testing setup was developed using an Infrared Systems Development IR-564/301 Black Body source [27] and optical table. Light was focused onto the sensing Photodiodes using a 50mm focal length lens.

The temperature of the Black Body source was then swept down from 1000°C in 100°C or 10°C steps (depending upon the granularity required to characterize the change in output). 30 or 15 minute intervals respectively were used to allow the source to settle between changes. At each temperature step, the output of the LIA was measured. An image of the setup characterizing the new design is shown in Appendix Fig. 19.

IV. Results & Evaluation

This section summarizes and evaluates the results from several tests aiming to characterize the performance of both the old [9] and new design of Lock-in Amplifier.

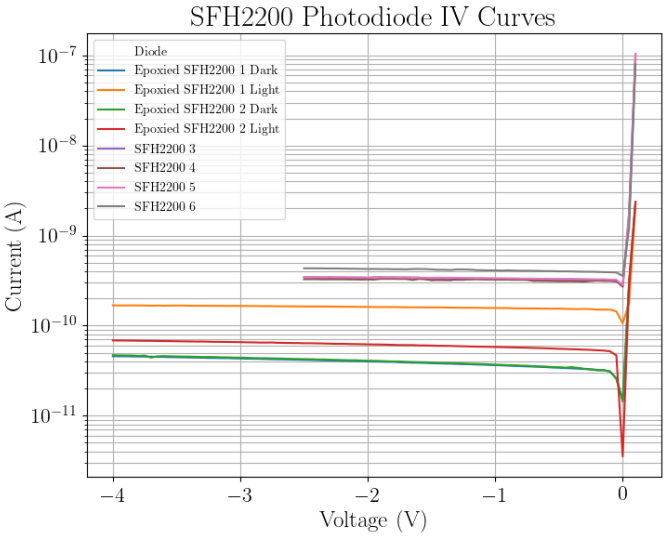

Figure 8: SFH2200 Photodiode IV Curves with epoxied diodes

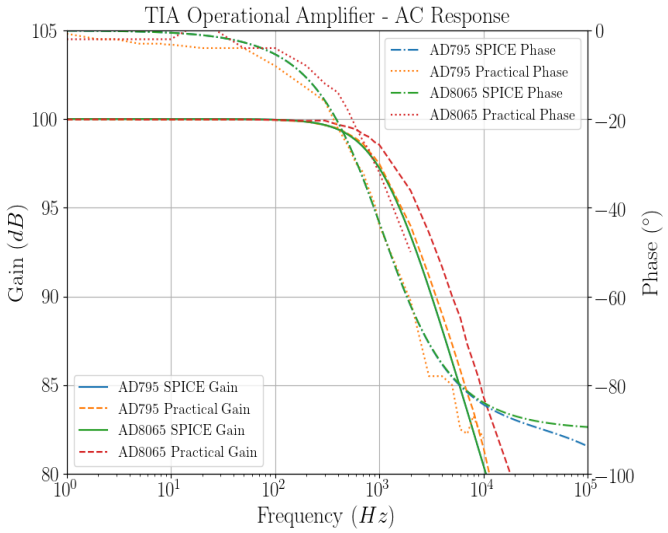

Figure 10: TIA Operational Amplifier candidate practical Frequency Response

A. *SFH2200 Photodiode IV Curves*

Fig. 8 shows the IV curves of a set of SFH2200 near Infrared Photodiodes. All diodes exhibit the expected shape for a logarithmic Y scale IV curve. It is important to note that the Y values have been converted to absolute values to ensure the logarithmic scale functions correctly.

All diodes have a dark current significantly lower than the specified maximum of 25nA from the manufacturer datasheet [16], with most in the 10s to 100s of pA range. The dark current value is very consistent between devices, with all diodes within an order of magnitude of each other.

Black epoxy was applied to two diodes to block out background light and provide a better dark current reference reading. The small difference in the diodes reverse bias current when illumination was switched on and off indicates this is an adequate method of covering the diodes.

B. *TIA Simulation and Testing*

Fig. 14, Fig. 15 (see appendices) and Fig. 9 show that the AD795 [28] exhibits the best combination of frequency response, linearity and noise.

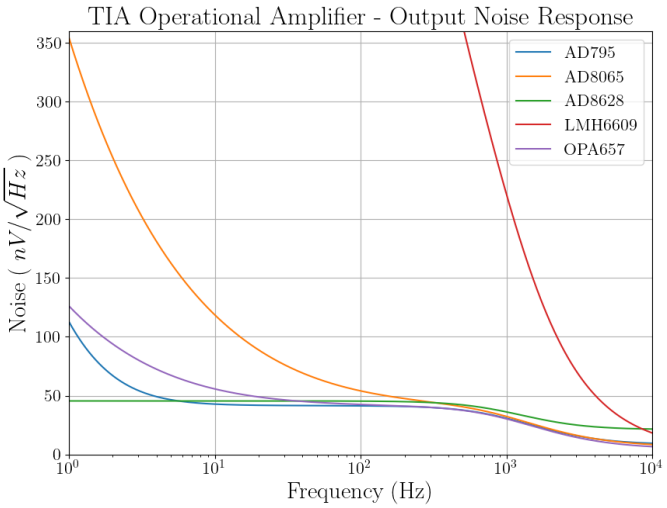

Figure 9: TIA Operational Amplifier candidate Output Noise Response

Additionally, the AD8065 [29] provides a reasonable low cost alternative with a higher gain bandwidth and slew rate, should they be required. Based upon the simulations and manufacturer reported characteristics, the AD795 and AD8065 were selected for practical testing.

Fig. 10 and Fig. 11 show the results of practical frequency response and linearity testing using the AD795 and AD8065 respectively. Due to access limitations for noise measurement equipment, it was not possible to take practical noise curves.

The practical results show that both devices accurately meet the 100k gain, 1kHz bandwidth specification. Additionally, both devices exhibit a linear response down to 100pA.

C. *Previous LIA Design Black Body Testing*

In order to provide a quantitative benchmark for the new Lock-in Amplifier design, a Black Body Radiation Thermometry test of the previous design was conducted. Starting at 1000°C, the temperature was stepped down by 100°C in 30-minute intervals. At each step the output of the LIA was measured using a multimeter.

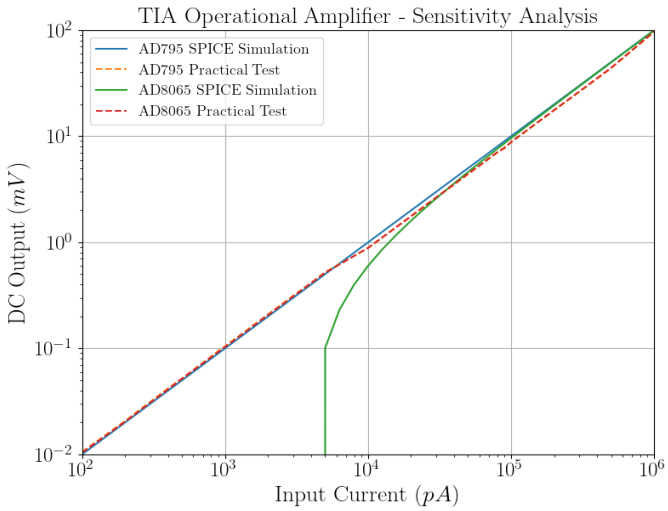

Figure 11: TIA Operational Amplifier candidate practical Linearity

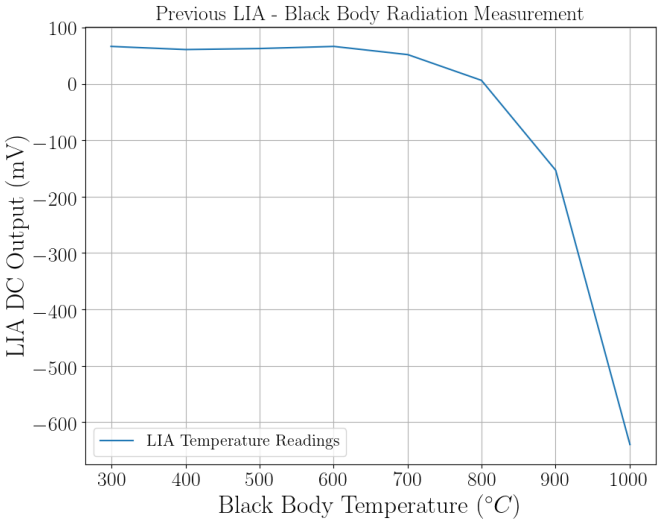

Figure 12: Previous LIA Design Black Body Radiation Testing

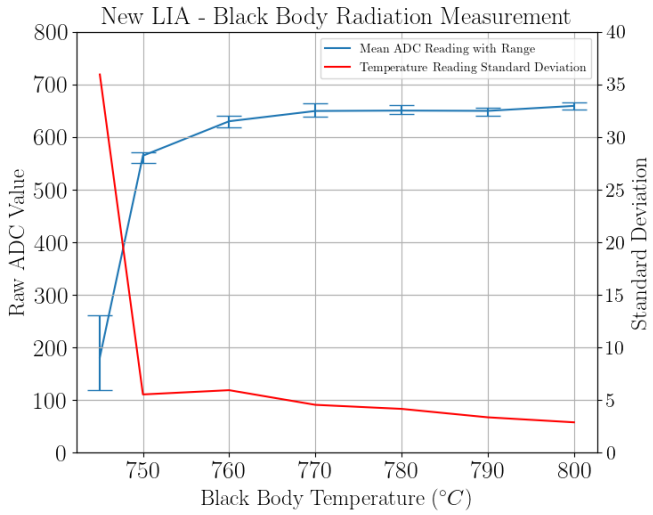

Figure 13: New LIA Design Black Body Radiation testing

Fig. 12 shows the results of the Black Body test. The curve indicates that the optical power of the Black Body increases exponentially with increasing temperature. Additionally, the previous design can comfortably measure a minimum temperature of 700°C. Table II shows the full set of results.

D. New LIA Design Black Body Testing

Fig. 13 shows the results from the Black Body Radiation Thermometry testing of the new LIA design. A sweep from 800°C to 745°C in 10°C steps was performed with 15-minute intervals. The LIA output was logged in 1 second intervals with a 30-point rolling average; a small logging interval helps capture short term irregularities in the output.

The mean ADC value curve indicates that the minimum temperature the new design can measure is 745°C. Below this value the ADC reading drops to 0. In juxtaposition to the previous LIA design, the new design produces an exponentially decreasing change in ADC reading with increasing temperature.

The error bars show the range of ADC values produced at the given temperature. The LIA exhibits approximately 4% of reading in noise at temperatures above 750°C; this equates to ±15°C error. This value increases as the temperature reaches the LIA's measurement threshold. This analysis is backed up by the standard deviation measurement.

V. Discussion

The low dark currents of 10s to 100s of pA shown in Fig. 8 indicate that the SFH2200 Photodiodes are a good selection for Infrared Radiation Thermometry. The consistency of the dark current value will reduce the error produced by differences in dark current of the sensing and reference diodes.

Additionally, Fig. 8 shows that covering the Photodiode with black epoxy is an adequate method of blocking light and limiting the output signal to the dark current.

Fig. 10 shows that the TIA design performs beyond specification, achieving 100k gain and 1kHz bandwidth with overhead to increase the gain up to a value of 10 Million.

Fig. 11 shows that the TIA design exhibits perfect linearity down to 100pA, a current lower than most Photodiode dark currents. The small step shift in linearity results is due to changes in the large resistance used to produce a current source to drive the TIA. The practical improvement in performance over the AD8065 simulated results is explained by the simulation producing a negative offset in output, leading to an infinite spike on the log Y scale graph. Fig. 15 exhibits similar behavior from the AD8628.

Fig. 9 shows that simulated noise levels across the entire frequency range are lower than 120nV/Hz$^{1/2}$ and 360nV/Hz$^{1/2}$ when using the AD795 and AD8065 respectively. Both the AD795 and AD8065 have a lower Input Noise Current when compared to the previous designs OPA656 [9]. Further practical noise testing to gain a real-world evaluation of these designs is required.

Thus, the new design provides similar performance to the previous design [9] at a lower operational amplifier cost of £7.53 (AD795) or £3.20 (AD8065) compared to £9.55 for the OPA656. Consequently, the AD8065 was selected for use in the new LIA design.

Black Body Radiation Testing of the new LIA design was carried out with a modulation frequency of 12.5kHz (100kHz input frequency, 8 times Clock Divider), with the modulated signal showing no square wave distortion. This indicates that the modulation circuit can operate at frequencies up to 12.5kHz as the ADG849 manufacturer datasheet quotes a maximum switching frequency of 18MHz [20]. As such, it is satisfactory for the LIA design and will allow for detailed testing of the optimal modulation frequency to use for Radiation Thermometry purposes.

Fig. 12 indicates the previous LIA design can measure to a minimum of 700°C. More granular experiments are required to find the exact minimum measurable temperature of the previous design. Given that most common high temperature sensors detect in a range of 400°C to 1000°C, there is room for improvement on this performance. Previous analysis shows that the old LIA produced a ±1mV stability of reading [9]. Results from the Black Body Radiation Thermometry testing setup, presented in Table II (data from Fig. 12), show

that the LIA exhibits approximately ±8mV or ±50°C stability of reading when measuring Infrared.

The exponential increase of LIA output with increasing temperature is explained by (1) and (2). As the temperature increases the wavelength of peak radiation decreases. This shifts it further into the detection range of the Photodiode, producing a larger output signal. Additionally, (2) shows that the Total Spectral Radiance emitted from the Black Body source increases with temperature to the power of 4.
Thus, each 100°C increase in temperature produces a LIA output several orders of magnitude higher than the last temperature step.

Fig. 13 shows that the minimum measurable temperature of the new LIA design is 745°C. Additionally, analysis of the range of measured values for a given temperature shows that the LIA produces an accuracy of ±15°C when measuring within the centre of its range. The calculation of this value was improved by digital logging through the PC Tool. This improvement over the ±50°C of the previous design is likely due to use of the ADA2200 (which provides a digital implementation of phase sensitive detection) and the Teensy's onboard 16 bit ADC, which provides more granular measurements than the ADC used in the previous design [9].

The displayed trend of LIA output flattening out with increasing temperature is in complete juxtaposition to the expected exponential increase. Bench testing showed that this was a result of the analogue switch significantly attenuating the modulated signal, resulting in a smaller reading from the LIA. Replacing the analogue switch remedied this problem. Due to the impact of COVID-19 on the project, a repeat Black Body Radiation Thermometry test was not possible.

Several other areas of the project remain incomplete due to the impact of the Coronavirus. Firstly, more granular measurements of the performance of both the old and new LIA design in Black Body Radiation Thermometry tests will give much greater insight into how much improvement has been made in the new design. These are yet to be completed.

Additionally, using additional external sources of Infrared Radiation that could be modulated at specific frequencies, the project had aimed to test frequencies that interfered with the Lock-in Amplifier. This would provide insight into the correct filters to use alongside the Lock-in Amplifier.

Finally, the project had intended to test the Lock-in Amplifier with a range of reference frequencies to ascertain the optimum value for Radiation Thermometry measurements.

VI. Conclusions

In conclusion, we can make the following comments about performance against the specification. Firstly, the suitability of Lock-in Amplifiers for Radiation Thermometry has been somewhat quantified through this project's experiments.

Fig. 12 and Fig. 13 clearly show that Electronic LIAs are capable of Radiation Thermometry measurements. Further experiments are required to evaluate the performance of LIAs in this field compared to the current industry standard.

Secondly, an amplification chain suitable for pA detection has been successfully produced, with an achievable maximum gain of 1 Billion. This was not possible with the TIA alone due to operational amplifier gain bandwidth limitations. Analysis contained within this report and the Interim Report [8] shows that the TIA and Inverting Amplifiers are very low noise with ideal linearity to 100pA. Thus, they are very suitable for the Radiation Thermometry application.

Finally, a new low-cost Electronic Lock-in Amplifier design (proof of concept) suitable for Radiation Thermometry has been constructed with suitable filters, as demonstrated in Fig. 13. Further testing is required to quantify the performance of this new design. As the attenuation produced by the analogue switch has been remedied, better performance than that shown in Fig. 13 is expected. The design is low-cost and small form factor, with a total production cost of approximately £90 and final dimensions of 11 x 8.3 x 3.5cm. At present, an SR830 Lock-in Amplifier with SR540 Optical Chopper costs approximately £5200 in a rack mount casing. The new design offers added functionality, such as software control and combined phase measurement.

The presented design is only a proof of concept. Consequently, it is not suitable for mass production or implementation in commercial systems. Further work is required to meet CE marking and electromagnetic interference standards. Nonetheless, this design shows that LIA technology can be produced at a low cost in a small form factor. This makes it much more accessible for industry, and could improve safety and system control in high temperature environments where accurate measurement is required.

Considering the effects of the Coronavirus Pandemic on the project timeline, this project has successfully met the minimum requirements and clearly outlined the path for future development. The produced LIA design is suitable to act as a platform for future development, with limited modifications required to make a very functional measurement instrument.

VII. Future Work

The following are recommendations for future work based upon the results of this project:

- Modifications to the LIA design to improve the dynamic range of the input. This may be achievable by implementing a software configurable TIA gain.
- Modifications to produce a software configurable Low Pass Filter alongside the configurable clock.
- Adaptation of the Lock-in Amplifier design for Gas Sensing applications, using infrared absorption techniques to ascertain the amount of gas present in a chamber.
- Adaptation of the Lock-in Amplifier design for use in a LIDAR system. As the PC Tool implements software communication with the LIA, readings produced by the tool could be used to build 3D point cloud scans of objects or environments.
- Adaptation of the Lock-in Amplifier design for use in long range optical communication systems where signal noise becomes a significant factor in speed.
- Exploration of producing a System on a Chip (SOC) equivalent of the Lock-in Amplifier design. This could be integrated with Photodiodes to produce modules for use in handheld devices such as Smartphones, Scanners and Temperature Probes.

References

[1] D. P. DeWitt, *Applications of Radiation Thermometry*. ASTM, 1985.

[2] P. Saunders, *Radiation Thermometry - Fundamentals and Applications in the Petrochemical Industry*. Bellingham, Washington 98227-0010 USA: SPIE, 2007.

[3] D. W. Ball, *Field guide to spectroscopy*. Bellingham, Wash.: SPIE Press, 2006.

[4] 'About Lock in Amplifiers'. Stanford Research Systems, Jan. 2020, Accessed: Jan. 08, 2020. [Online]. Available: https://www.thinksrs.com/downloads/pdfs/applicationnotes/AboutLIAs.pdf.

[5] 'SR830 Lock in Amplifier Manual'. Stanford Research Systems, Oct. 2011, [Online]. Available: https://www.thinksrs.com/downloads/pdfs/manuals/SR830m.pdf.

[6] P. Horowitz, *The Art of Electronics*, Third edition. New York, NY: Cambridge University Press, 2015.

[7] 'Stanford Research Systems SR810 and SR830 Lock in Amplifiers', *Stanford Research Systems*, Jan. 2020. https://www.thinksrs.com/products/sr810830.html.

[8] S. Maxwell, 'Electronic Lock-in Amplifier for Low Cost Radiation Thermometry - Interim Report', The University of Sheffield, Electrical and Electronic Engineering Department, Sheffield, Technical, Jan. 2020. Accessed: Mar. 25, 2020. [Online]. Available: https://drive.google.com/file/d/1F94Ycx0VlRlgqeq8cT8joeFJ9Hxp3Jm0/view.

[9] T. Osman, 'Electronic Lock-In Amplifier for Measuring Low Optical Power', *Univ. Sheff.*, 2019, [Online]. Available: https://drive.google.com/drive/u/0/folders/1mKkyF--GX4QIbBFBThfYsIP8hpdrWZup.

[10] Analog Devices, 'LT SPICE', *LT SPICE Design Center*, Jan. 2020. https://www.analog.com/en/design-center/design-tools-and-calculators/ltspice-simulator.html.

[11] A. Auckloo, R. Tozer, J. David, and C. H. Tan, 'A low noise op-amp transimpedance amplifier for LIDAR applications', presented at the 21st IEEE International Conference on Electronics, Circuits and Systems (ICECS), NJ, Dec. 2014.

[12] G. Hutton, 'Full-fibre broadband in the UK', House of Commons Library, Briefing Paper CBP 8392, Jan. 2020. Accessed: Mar. 26, 2020. [Online]. Available: http://researchbriefings.files.parliament.uk/documents/CBP-8392/CBP-8392.pdf.

[13] P. Koutroumpis, 'The economic impact of broadband: evidence from OECD countries.', OFCOM, Briefing Paper, Apr. 2018. [Online]. Available: https://www.ofcom.org.uk/__data/assets/pdf_file/0025/113299/economic-broadband-oecd-countries.pdf.

[14] 'Tesla Autopilot crash driver "was playing video game"', *BBC News*, London, Feb. 26, 2020.

[15] J. Allison, *Electronic engineering semiconductors and devices*, 2nd ed. London ; New York: McGraw-Hill, 1990.

[16] O. Opto Semiconductors, 'SFH 2200 Datasheet'. Jun. 23, 2017, [Online]. Available: https://dammedia.osram.info/media/resource/hires/osram-dam-5970058/SFH%202200_EN.pdf.

[17] G. Giusi, G. Cannatà, G. Scandurra, and C. Ciofi, 'Ultra-low-noise large-bandwidth transimpedance amplifier: ULTRA-LOW-NOISE LARGE-BANDWIDTH TRANSIMPEDANCE AMPLIFIER', *Int. J. Circuit Theory Appl.*, vol. 43, no. 10, pp. 1455–1473, Oct. 2015, doi: 10.1002/cta.2015.

[18] Analog Devices, 'ADA2200 Synchronous Demodulator Datasheet'. Analog Devices, Accessed: Jan. 12, 2020. [Online]. Available: https://www.analog.com/media/en/technical-documentation/data-sheets/ADA2200.pdf.

[19] Linear Technology, 'LT1007 Operational Amplifier Datasheet'. Linear Technology, Accessed: Jan. 11, 2020. [Online]. Available: https://www.analog.com/media/en/technical-documentation/data-sheets/LT1007-LT1037.pdf.

[20] Analog Devices, 'ADG849 Analogue Switch Datasheet'. Analog Devices, 2004, Accessed: Mar. 29, 2020. [Online]. Available: https://www.analog.com/media/en/technical-documentation/data-sheets/ADG849.pdf.

[21] PJRC, 'Teensy 3.2 Datasheet'. PJRC, 2019, Accessed: Jan. 13, 2020. [Online]. Available: https://www.pjrc.com/teensy/card7a_rev1.pdf.

[22] Texas Instruments, 'LM2937 Linear Voltage Regulator Datasheet'. Texas Instruments, 2014, Accessed: Jan. 13, 2020. [Online]. Available: http://www.ti.com/lit/ds/symlink/lm2937.pdf.

[23] W. Stambaugh, 'KiCAD PCB Design Software', 2019. https://kicad-pcb.org/ (accessed Jan. 13, 2020).

[24] P. C. D. Hobbs, *Building electro-optical systems: making it all work*, 2nd ed. Hoboken, N.J: Wiley, 2009.

[25] S. Maxwell, 'LIA - Remote Communication Protocol Guide'. Feb. 14, 2020, Accessed: Mar. 29, 2020. [Online]. Available: https://docs.google.com/document/d/1Cgs6-552I8XdlsIetVLS-LEy0_qNMW5MgRgujQ0Im4Y/edit.

[26] S. Maxwell, 'EEE381 Lock-in Amplifier Github Repository'. Electrical and Electronic Engineering Department at the University of Sheffield, Accessed: Mar. 29, 2020. [Online]. Available: https://github.com/TehMaxwell/EEE381-Assignment.

[27] Infrared Systems Development, 'IR-564/301 Blackbody System Webpage'. Mar. 30, 2020, [Online]. Available: https://www.infraredsystems.com/Products/blackbody564.html.

[28] Analog Devices, 'AD795 Operational Amplifier Datasheet'. Analog Devices, 2019, Accessed: Jan. 11, 2020. [Online]. Available: https://www.analog.com/media/en/technical-documentation/data-sheets/ad795.pdf.

[29] Analog Devices, 'AD8065 Operational Amplifier Datasheet'. Analog Devices, 2019, Accessed: Jan. 11, 2020. [Online]. Available: https://www.analog.com/media/en/technical-documentation/data-sheets/AD8065_8066.pdf.

APPENDICES

Component Name	GBW (MHz)	Slew Rate (V/µs)	Input Noise Current (pA/Hz$^{1/2}$)	Input Noise Voltage (nV/Hz$^{1/2}$)	Input Offset Voltage (µV)	Cost (£)
OPA657	1600	700	0.0013	4.8	250	10.16
AD8065	145	180	0.0006	7	1500	3.20
AD795	1.6	1	0.0006	9	500	7.53
LMH6609	260	1400	1.6	3.1	2500	2.45
AD8628	2.5	1	0.005	22	5	3.04

TABLE I
TIA Candidate Operational Amplifiers

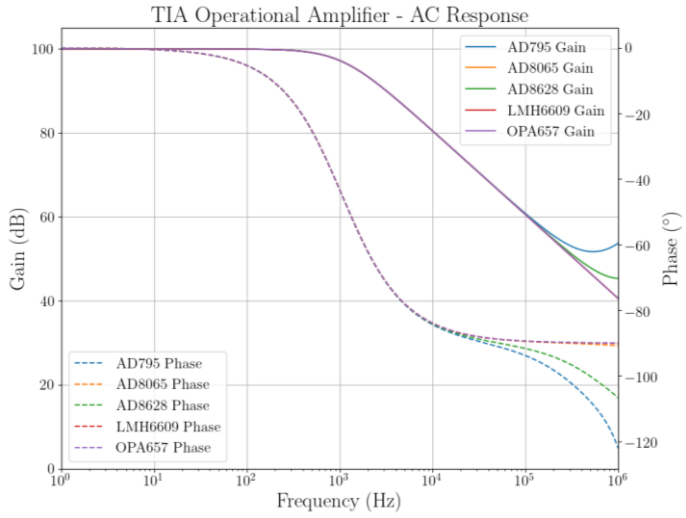

Figure 14: TIA Operational Amplifier candidate Frequency Response

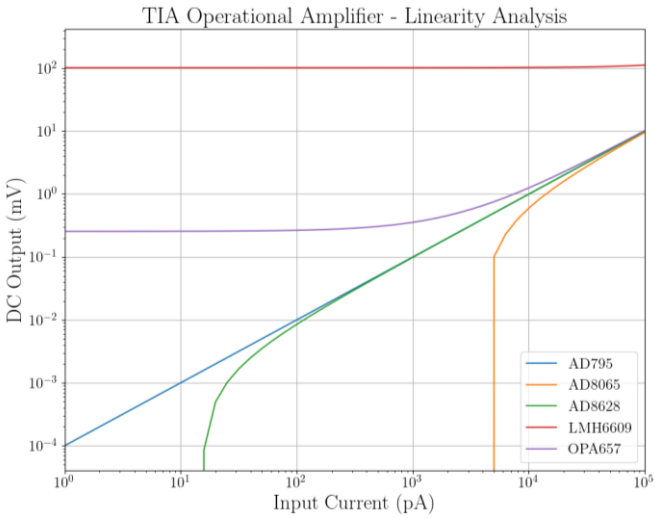

Figure 15: TIA Operational Amplifier candidate Linearity Response

Temperature (°C)	Reading 1 (mV)	Reading 2 (mV)	Reading 3 (mV)	Reading 4 (mV)	Reading Range (mV)
1000.6	-640.0	-	-	-	-
900.2	-153.0	-	-	-	-
799.9	6.0	3.7	9.1	7.6	5.4
700.4	52.0	49.8	56.0	51.4	6.2
600.4	65.8	62.1	69.3	70.3	8.2
500.2	60.6	62.7	64.1	65.2	4.6
400.0	59.2	60.4	61.7	64.0	4.8
299.0	64.2	65.1	70.2	68.1	6.0

TABLE II
Previous Lock-in Amplifier Black Body Radiation Thermometry Testing Results

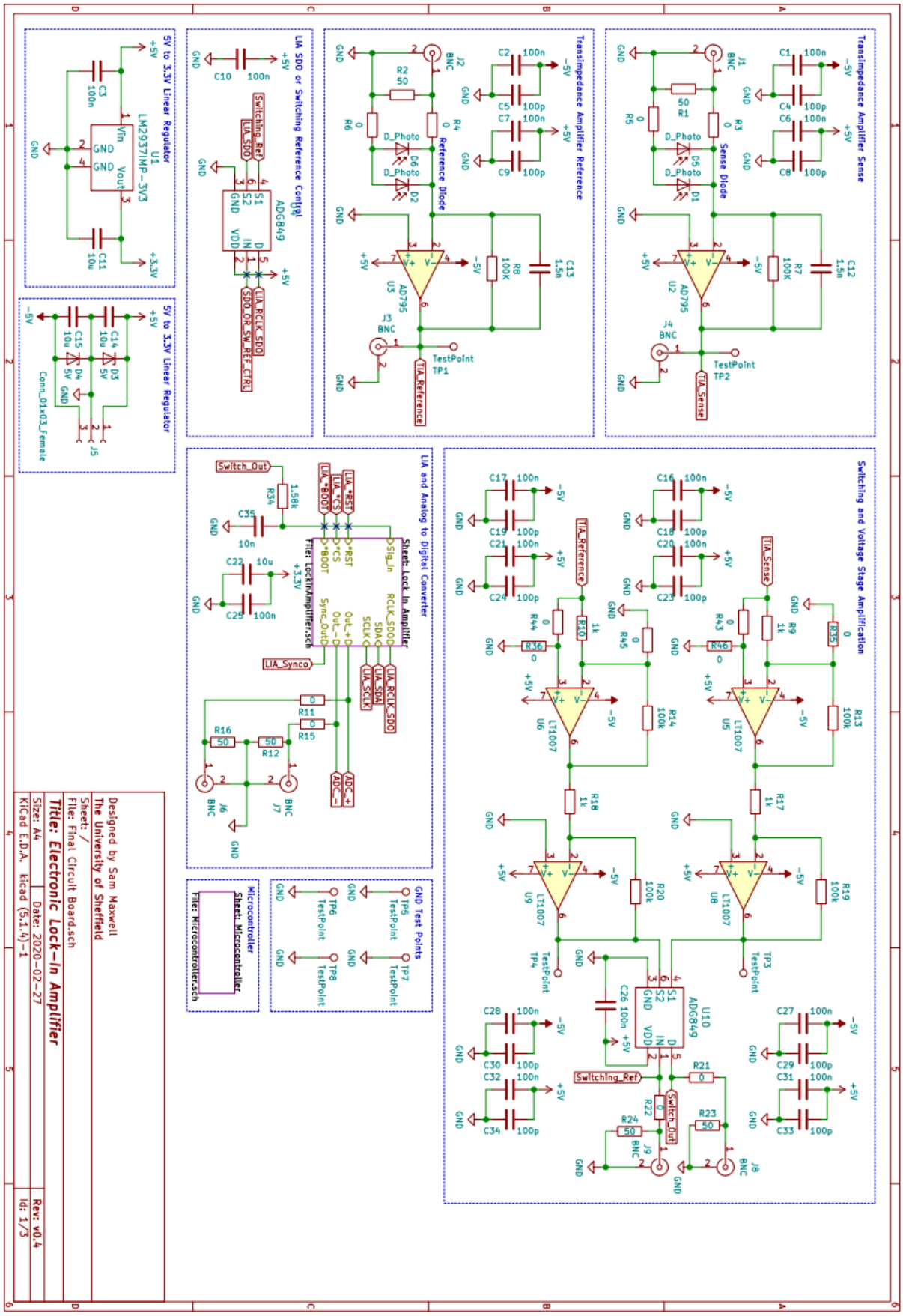

Figure 16: Completed Electronic Lock-in Amplifier Schematic

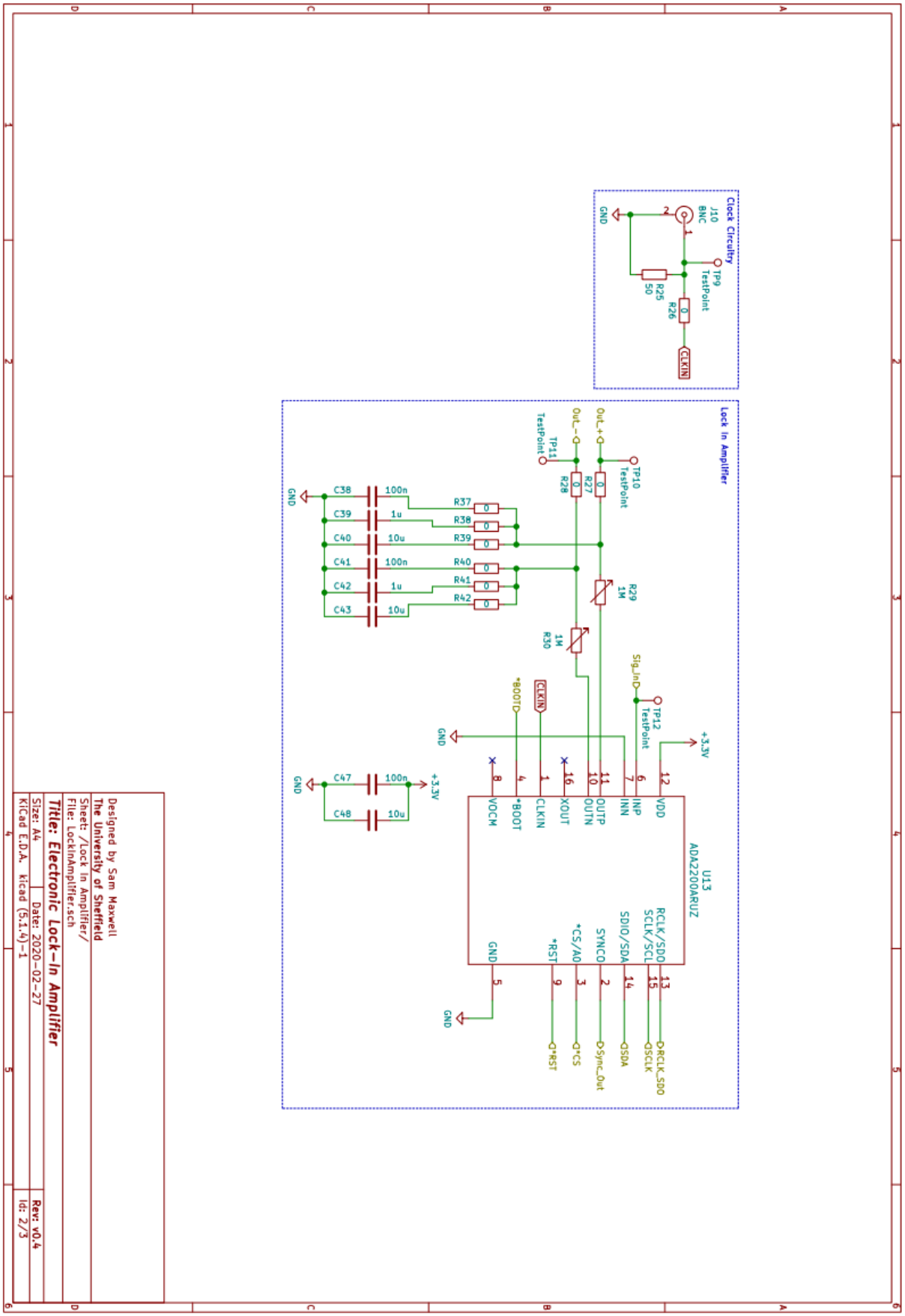
Clock Circuitry
J10
BNC
TP9
TestPoint
R25
50
R26
0
CLKIN
GND
Lock In Amplifier
Out_+
Out_-
TP10
TestPoint
TP11
TestPoint
R27
0
R28
0
R29
1M
R30
1M
C38
100n
C39
1u
C40
10u
C41
100n
C42
1u
C43
10u
R37
0
R38
0
R39
0
R40
0
R41
0
R42
0
SigInD
TP12
TestPoint
*BOOTD
CLKIN
+3.3V
C47
100n
C48
10u
U13
ADA2200ARUZ
VDD
INP
INN
OUTP
OUTN
XOUT
CLKIN
*BOOT
VOCM
GND
RCLK/SDO
SCLK/SCL
SDIO/SDA
SYNCO
*CS/A0
*RST
RCLK_SDO
SCLK
SDA
Sync_Out
*CS
*RST
Designed by Sam Maxwell
The University of Sheffield
Sheet: /Lock In Amplifier/
File: LockInAmplifier.sch
Title: Electronic Lock-In Amplifier
Size: A4
Date: 2020-02-27
KiCad E.D.A. kicad (5.1.4)-1
Rev: v0.4
Id: 2/3

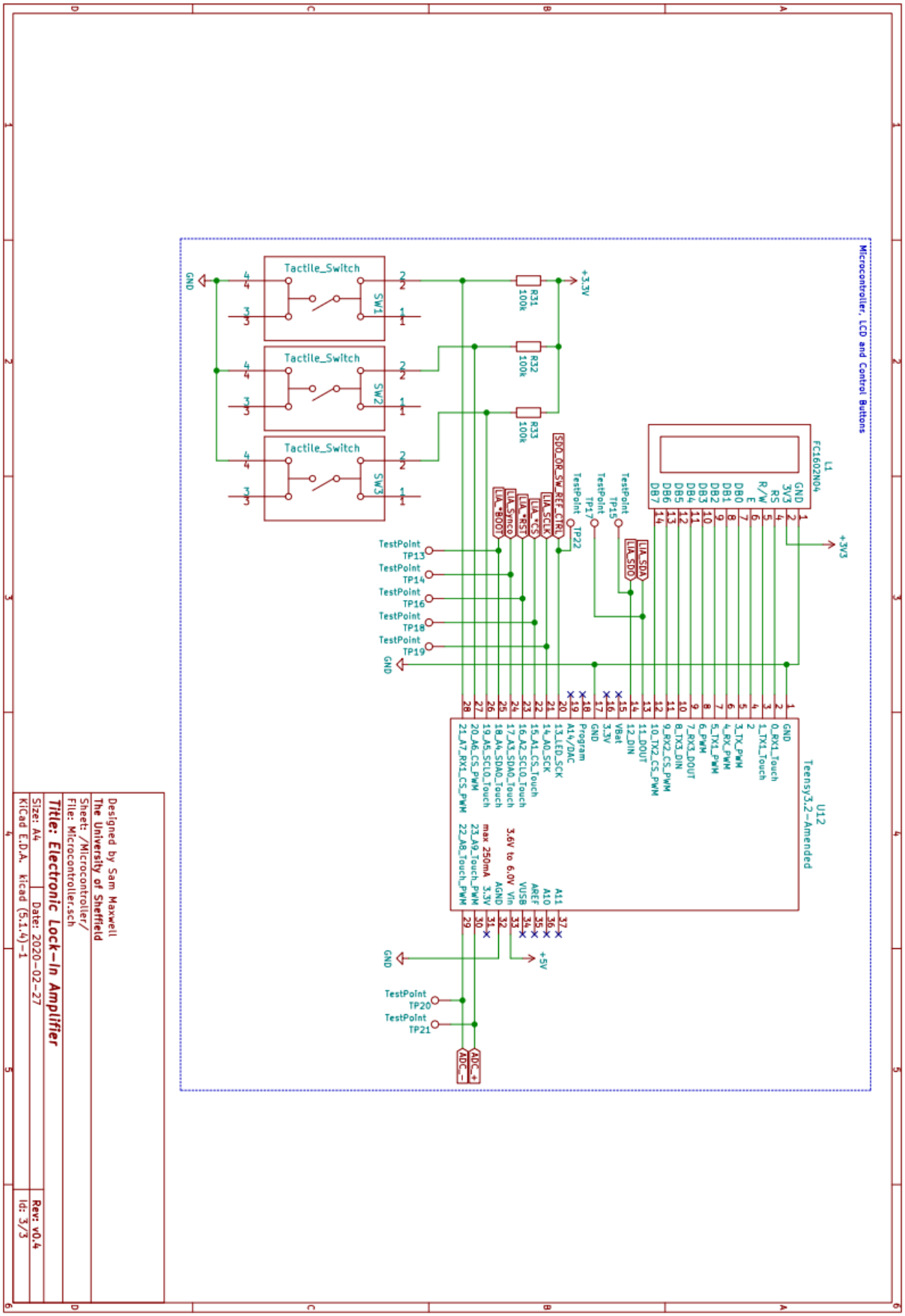
Microcontroller, LCD and Control Buttons
Tactile_Switch
SW1
SW2
SW3
R31 100k
R32 100k
R33 100k
+3.3V
GND
SDO_OR_SW_REF_CTRL
LIA_SCLK
LIA_~CS
LIA_~RST
LIA_Sync
LIA_~BOOT
LIA_SDA
LIA_SDO
TestPoint
TP13
TP14
TP16
TP17
TP18
TP19
TP20
TP21
TP22
L1
FC1602NQ4
+5V
U12
Teensy3.2-Amended
3.6V to 6.0V
max 250mA
ADC+
ADC-
Designed by Sam Maxwell
The University of Sheffield
Sheet: /Microcontroller/
File: Microcontroller.sch
Title: Electronic Lock-In Amplifier
Size: A4
Date: 2020-02-27
KiCad E.D.A. kicad (5.1.4)-1
Rev: v0.4
Id: 3/3

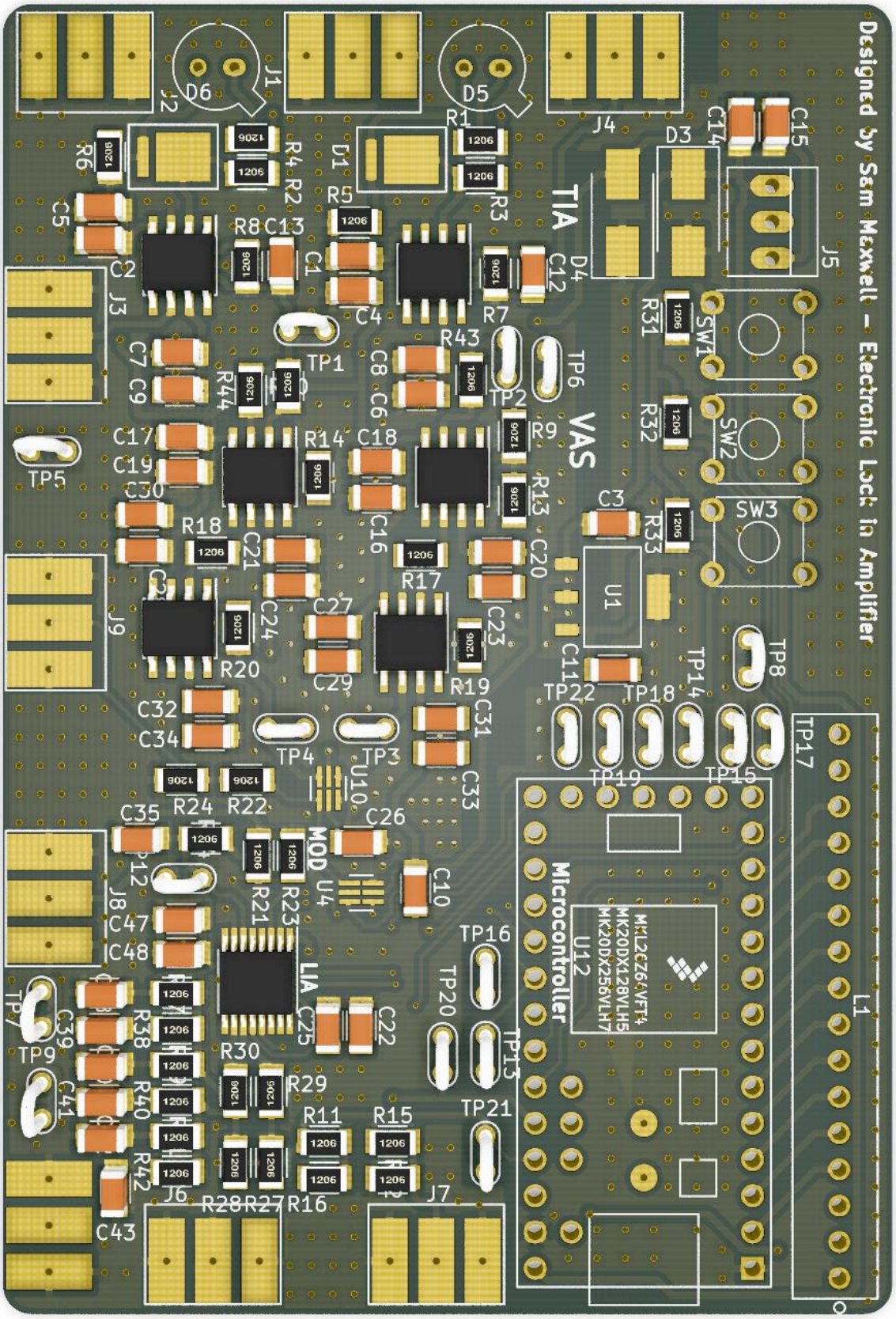

Figure 17: Completed Lock-in Amplifier PCB 3D Render

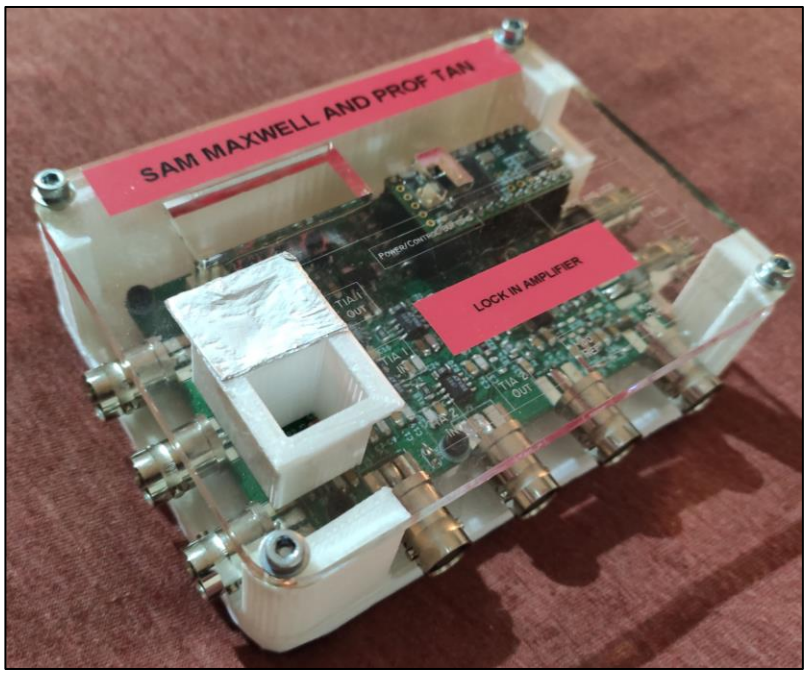

Figure 18: Final LIA PCB and Casing with Light Guide

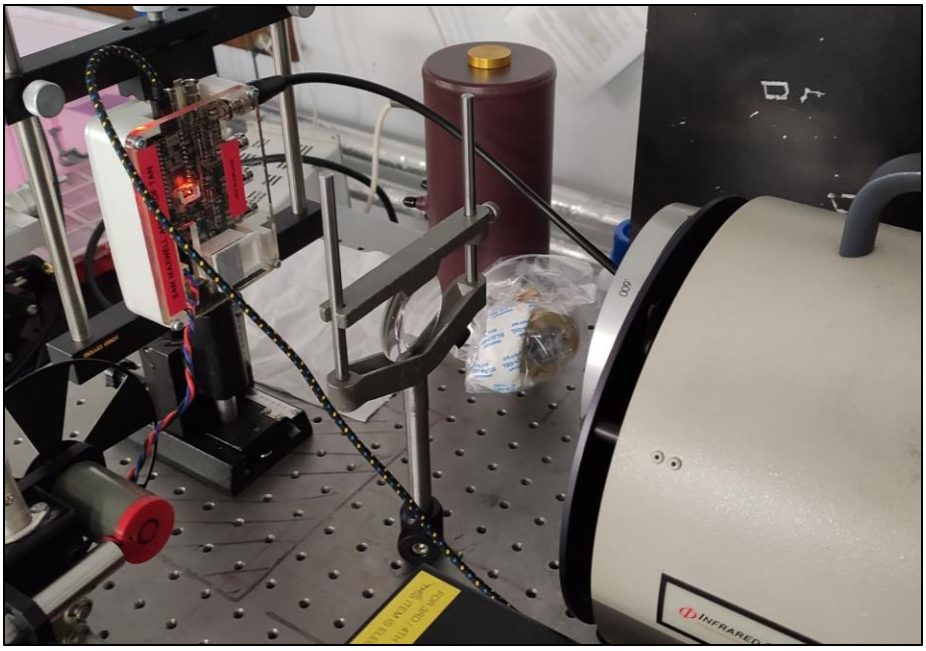

Figure 19: Black Body Radiation Thermometry Testing Setup with new LIA Design